

## Article

# Seismic Pile–Soil Interaction Analysis Based on a Unified Thixotropic Fluid Model in Liquefiable Soil

Xinlei Zhang <sup>1,2</sup>, Zhanpeng Ji <sup>1,2</sup>, Jun Guo <sup>1,2</sup>, Hongmei Gao <sup>1,2,\*</sup> and Zhihua Wang <sup>1,2</sup><sup>1</sup> Urban Underground Space Research Center, Nanjing Tech University, Nanjing 210009, China<sup>2</sup> Institute of Geotechnical Engineering, Nanjing Tech University, Nanjing 210009, China

\* Correspondence: hongmei54@njtech.edu.cn

**Abstract:** One of the challenges to the analysis of interactions between soil and piles in lateral spreading is the modeling of the progress generated by excess pore pressure and soil strength and stiffness degradation. In this paper, a pile–soil interaction analysis method that introduces the thixotropic-induced excess pore pressure model (TEPP) to describe the progressive development of the stress–strain rate connection of liquefying soil is proposed. The reliability of the method was verified by comparing the calculated results with that of the shake table test. Then, the parametric analyses of soil–pile interactions were carried out. The results show that the bending moment and horizontal displacement of pile foundations increase with the increase in superficial viscosity and inclination angle of the site. The horizontal dislocation and bending moment of the pile foundation increase with the decrease in loading frequency as a result of the property of amplifying low-frequency loads and filtering high-frequency loads of liquefied soil.

**Keywords:** fluid mechanics; sand liquefaction; non-Newtonian fluid; fluid–structure coupling; pile–soil interaction



**Citation:** Zhang, X.; Ji, Z.; Guo, J.; Gao, H.; Wang, Z. Seismic Pile–Soil Interaction Analysis Based on a Unified Thixotropic Fluid Model in Liquefiable Soil. *Sustainability* **2023**, *15*, 5345. <https://doi.org/10.3390/su15065345>

Academic Editors: Pengjiao Jia, Peixin Shi, Cheng Cheng and Xi Jiang

Received: 21 October 2022

Revised: 18 February 2023

Accepted: 13 March 2023

Published: 17 March 2023



**Copyright:** © 2023 by the authors. Licensee MDPI, Basel, Switzerland. This article is an open access article distributed under the terms and conditions of the Creative Commons Attribution (CC BY) license (<https://creativecommons.org/licenses/by/4.0/>).

## 1. Introduction

Pile foundations are extensively applied as the base of bridges, high-rise buildings, ports, and wharves due to their bearing capacity and small settlement. Earthquake liquefaction has a great influence on infrastructure such as structures and buildings and has become a hot research topic. The pile foundations of existing buildings and structures have been severely injured by liquefaction-induced lateral spreading during several earthquakes [1–3]. In the 1964 Niigata earthquake, the famous Showa Bridge caved because of liquefaction-induced lateral displacement [4]. The large lateral displacement of soil liquefaction resulted in severe damage to many pile-supported bridges and buildings in the 1976 Tangshan earthquake [5] and 2008 Wenchuan earthquake [6–8]; the liquefaction of foundational soil causes the shear failure and dislocation of pile foundations and the fracture and collapse of bridge decks. Consequently, serious attention should be paid to the seismic response analyses of pile foundations in sites susceptible to lateral spreading in an attempt to properly design the pile foundation and avoid potential damages. Therefore, based on the above data on pile foundation failure caused by the liquefaction of foundation soil, it is necessary to study the interaction mechanism between piles and liquefied soil.

The stiffness and shear strength of soil gradually decrease because of the excess pore water pressure generation caused by seismic loading, which may cause excessive shear deformation. After seismic loading, the flow deformation of liquefiable soils may continue under gravity loading, resulting in ground susceptibility to large flow deformation [9]. During the 1989 Tajik earthquake, the ground slid nearly 2 km due to liquefaction [10]. Many shake table tests [11–13], centrifuge model tests [14,15], and field tests [16] have been carried out to improve the understanding of seismic pile–soil interactions in lateral spreading. These tests mainly focus on soil pressure on the pile side [17], the inertial force

of the superstructure, the  $p$ - $y$  curve of the liquefiable site, and the influence of the upper non-liquefied layer on the response of single piles and group piles [18]. Broms et al. [19] proposed a method for calculating the horizontal bearing capacity of a single pile based on the assumption of homogeneous soil. However, the Broms method ignores the apparent cohesion of coarse-grained soil, and the calculation of coarse-grained soil is conservative. Hamada et al. [20] proposed that the large lateral displacement caused by soil liquefaction was the main reason for the injury of dams, underground structures, and other structures in the earthquake. Since then, the large lateral displacement of liquefied soil has resulted in a new understanding of the injury mechanism of pile foundations. Wang Ming-wu et al. [21] studied the seismic response of piles in a liquefied site with slope angles by using centrifuge tests. The test results showed that the lateral displacement of piles in a liquefied site with slope angles was more obvious than that in a horizontal liquefied site, and it was found that the lateral deformation of sand caused by seismic liquefaction increased the load borne by piles. The dynamic response of pile foundations in liquefied sites is still a complex problem.

The large deformation of the ground caused by liquefaction is the main cause of pile foundation failure during earthquakes. Compared with liquefaction itself, the large deformation caused by liquefaction may be more serious. Previous studies on liquefaction have focused on liquefaction prediction and its influencing factors. Recently, attention has been paid to the importance of large liquefaction deformation. These studies usually use traditional solid-mechanics-based methods and assume relatively limited shear deformation. However, compared with liquefaction itself, large deformations caused by liquefaction may be more serious relative to pile foundations. The strain of liquefied soil may exceed 100%; that is, the soil has changed from a solid phase to a fluid phase. Due to the existence of phase transitions, the behavior of liquefied soil is no longer suitably described by traditional elastoplastic constitutive models, which assume relatively limited shear deformation. Therefore, a new analytic method is necessary.

The application of the fluid dynamics method to analyze the dynamic pile–soil interaction is a new research idea. Computational fluid dynamics (CFD) is a computational method for finding discrete numerical solutions to various complex problems in fluid dynamics. In recent years, a preliminary attempt has been made to further CFD to solve liquefaction-related problems [22]. In this paper, a pile–soil interaction analysis method that introduces the thixotropic-induced excess pore pressure model (TEPP) to characterize the properties of liquefied soil is proposed. The method proposed in this paper was utilized for analyzing the large-scale shake table test of pile foundations in liquefied sites, and the reliability of the method was verified. The effect of the elastic modulus of piles, the superficial viscosity of soil, the inclination angle of the site, and the loading frequency on the dynamic response of pile foundations were discussed.

## 2. Fluid Model and Control Equation

According to the post-compression thixotropic fluid constitutive model, the liquefied soil is regarded as a non-Newtonian fluid, and the pile foundation is regarded as a linearly elastic solid. Therefore, the liquefied soil and pile satisfy the governing equations of fluids and linear elastic solids, respectively.

### 2.1. Constitutive Model of the TEPP Model

Under cyclic loading, the meso-structure of liquid soil changes. It is assumed that the skeleton composed of solid particles of soil is the internal network structure of fluid. Under the action of continuous earthquakes, the vibration pore water pressure increases continuously, and the internal structure is destroyed continuously and finally tends to the limit equilibrium state. From the perspective of thixotropic fluid, the liquefaction process of soil is described as a process in which an imaginary fluid with an initial equilibrium state gradually destroys the internal structure under cyclic shear and tends to a limit equilibrium state. Wang et al. [23] proposed the TEPP model for liquefiable soil, which can

properly capture the strain rate correlation before and during liquefaction. The TEPP model is adopted as the fluid constitutive relation to describe the rate-dependent behavior of liquefied soil in this research. Before cyclic loading, the soil skeleton of the liquefiable soil is in an intact and steady condition, which is defined as the initial equilibrium state, as shown in Figure 1, with  $r_u = 0$  and  $\lambda = 1$ . The continuous cyclic loading induces the generation of excess pore water pressure and the incremental failure of the internal structure. When the internal construction is completely destroyed, the soil is at a perfect liquefaction state, with  $r_u = 1$  and  $\lambda = 0$ , which means that it entered the limit equilibrium state (Figure 1).

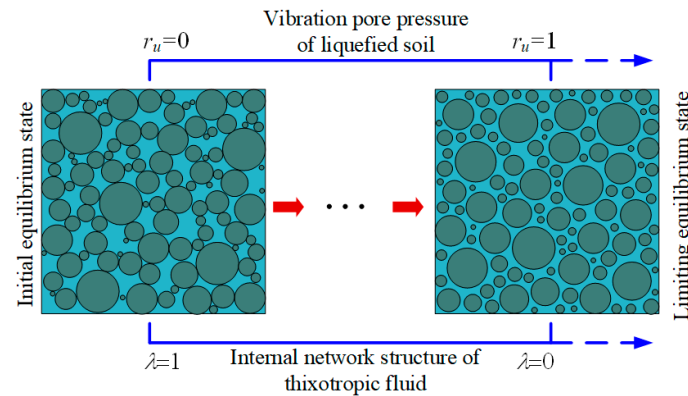


Figure 1. Concept of the TEPP fluid model.

Letting the  $\lambda = 1 - r_u$  state equation be consistent with the form of Moore-type thixotropic fluids and conform to the experimental results and two equilibrium states, the unified thixotropic fluid constitutive model of liquefiable soil is established based on the Moore-type thixotropic fluid constitutive equation. The state equation and velocity equation can be expressed as follows [24]:

$$\text{state equation : } \tau = [\eta_e + (\eta_\infty - \eta_e)]\dot{\gamma} \tag{1}$$

$$\text{velocity equation : } d\lambda/dt = b(1 - \lambda) - c\lambda\dot{\gamma} \tag{2}$$

where  $\eta_e$  is the viscosity factor in the limit equilibrium state (liquefaction),  $\eta_\infty$  is the viscosity factor in the initial state,  $b(1 - \lambda)$  and  $-c\lambda$  are the reconstruction and destruction of the soil internal network structure, and  $b$  and  $c$  are the physical parameters denoting the internal structure reconstruction rate and destruction rate, respectively.

### 2.2. Control Equation of Pile

The governing equation of pile vibration and displacement induced by the soil is as follows:

$$M \frac{d^2 y}{dt^2} + C \frac{dy}{dt} + Ky + \tau = 0 \tag{3}$$

where  $M$  is the mass matrix,  $C$  is the damping matrix,  $K$  is the stiffness matrix,  $y$  is the pile displacement, and  $\tau$  is the pile stress.

### 2.3. Coupling Interface Equation and Free Surface

The fluid–structure interaction interface needs to meet two basic conditions, that is, the kinematic and dynamic conditions. The kinematic conditions (displacement coordination) are expressed as follows:

$$y_f = y_s \tag{4}$$

Dynamic conditions (equilibrium of forces):

$$n\tau_f = n\tau_s \tag{5}$$

where  $n$  is the normal vector of the fluid–solid coupling interface,  $y_s$  is the structural displacement,  $y_f$  is the fluid displacement,  $\tau_s$  is the stress of the structure, and  $\tau_f$  is the fluid stress.

The contact surface between liquefiable soil and the atmosphere is free, and its kinematic condition is as follows:

$$\frac{\partial F}{\partial t} + u \cdot \nabla F = 0 \quad (6)$$

where  $F$  represents all the physical quantities on the free surface. When the surface tension is not considered, the free surface pressure should satisfy  $P = P_a$ , and  $P_a$  is the atmospheric pressure.

### 3. Numerical Model for Shake Table Tests

In this research, liquefied sand is considered to be incompressible non-Newtonian fluid. Due to the great difference between the two materials, the contact surface between the pile and the liquefied soil may produce a staggered slip under certain stress conditions. Therefore, the coupling contact surface should be set here. According to the above principle, the iterative coupling method based on Adina finite element software is used to analyze the pile–soil interaction during soil liquefaction, and the bending moment distribution and displacement of the pile foundation are calculated and analyzed.

#### 3.1. Geometric Models and Boundary Conditions

The numerical analysis of Model 1 in the large shake table tests conducted by He et al. [25] was carried out to verify the proposed method in this study. The physical model profile and sensor arrangement of Model 1 are shown in Figure 2. An inclined layered shear box with  $11.6 \text{ m} \times 3.5 \text{ m} \times 6 \text{ m}$  (length  $\times$  width  $\times$  thickness) was used to model a gentle slope with an inclination angle of 2 degrees. The piles used in the test were 5.8 m long in total, with a length of 5 m buried in the soil. Two kinds of end-bearing piles, with pipe thicknesses of 6 mm and 3 mm, respectively, were used in the tests to inquire into the effect of pile stiffness. The water table was 5 m high from the bottom of the container. To achieve liquefaction in shake table tests, the relative density of sand was controlled to be 40~50%. Experiments were conducted using a sinusoidal base excitation with an acceleration amplitude of 0.2 g, frequency of 2 Hz, and duration of 10 s. The time history of input dynamic loading is given in Figure 3.

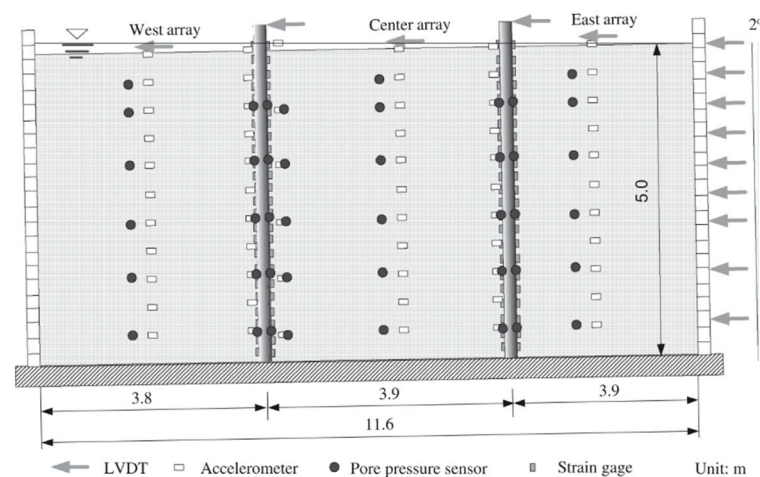


Figure 2. Sketch of shake table test and sensor setup (Model 1 [25]).

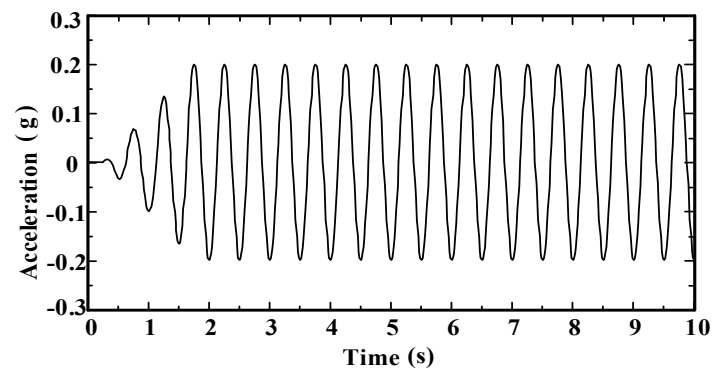


Figure 3. The input signal of sine wave.

The dimensions of the numerical model were set to be exactly the same as the physical model. The pile structure and surrounding soil were meshed by the eight-node hexahedron elements and FCBI elements (flow-condition-based interpolation) [26], respectively, as shown in Figure 4. For the solid domain, the left and the right boundary of the model were free to move in the shaking direction due to the layered shear box, while the out-of-plane displacement was constrained by the front, back, and bottom boundaries. For the fluid domain, the left and right boundaries were set to zero velocity in the shaking direction, the front and back boundaries were set to be solid wall boundaries, and the surface was set to free liquid surface. The pile end was fixed on the bottom of the model.

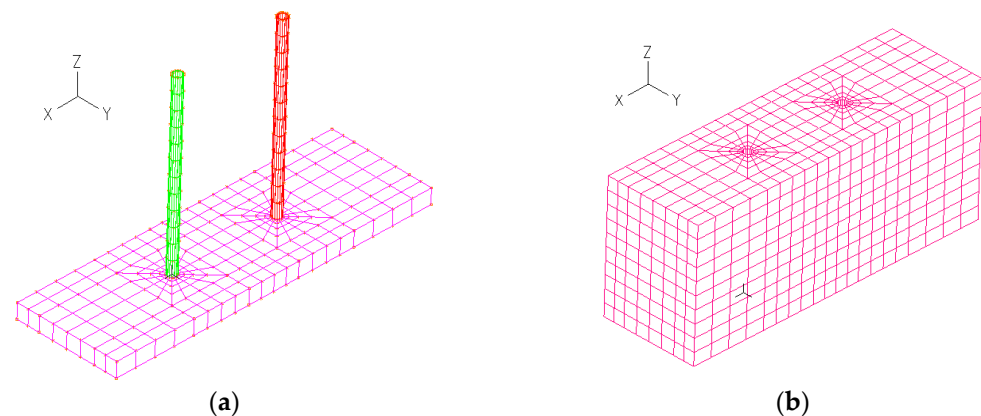


Figure 4. Mesh of numerical model for shake table test. (a) The structural domains. (b) The soil domains.

There was a possibility of misaligned slips on the contact surface between the pile and the liquefiable soil under a certain stress condition, and a coupling contact surface was applied in this study.

### 3.2. Material Parameters

The pile is considered a linearly elastic material, and liquefied soil is regarded as an incompressible non-Newtonian fluid. The specific parameters are listed in Table 1.

Table 1. Parameters of soil and pile foundation in the numerical model.

Projects	Length/ Thickness	Outer Diameter	Wall Thickness	Modulus of Elasticity	Density	Poisson's Ratio	Viscosity
	$h$ (m)	$d$ (m)	$\delta$ (m)	$E$ (GPa)	$\rho$ (kg/m <sup>3</sup> )	$\nu$	$\eta$ (kPa·s)
Rigid piles	5.8	0.318	0.006	200	7800	0.29	/
Flexible piles	5.8	0.318	0.003	200	7800	0.29	/
Liquefied Soil	5	/	/	/	1900	/	60~2000

For the soil domain, the TEPP is introduced, and the state equation is described in Equation (1). In this study, the coefficient of viscosity,  $\eta_{\infty}$ , of the liquefiable soil ranges from 60 kPa·s to 2000 kPa·s depending on the completeness of its internal structure, which could be indicated by the generation of excess pore pressure ratio in the soil. The relationship between the coefficient of viscosity and excess pore pressure ratio ( $u/\sigma'_c$ ) adopted in this study is given in Figure 5.

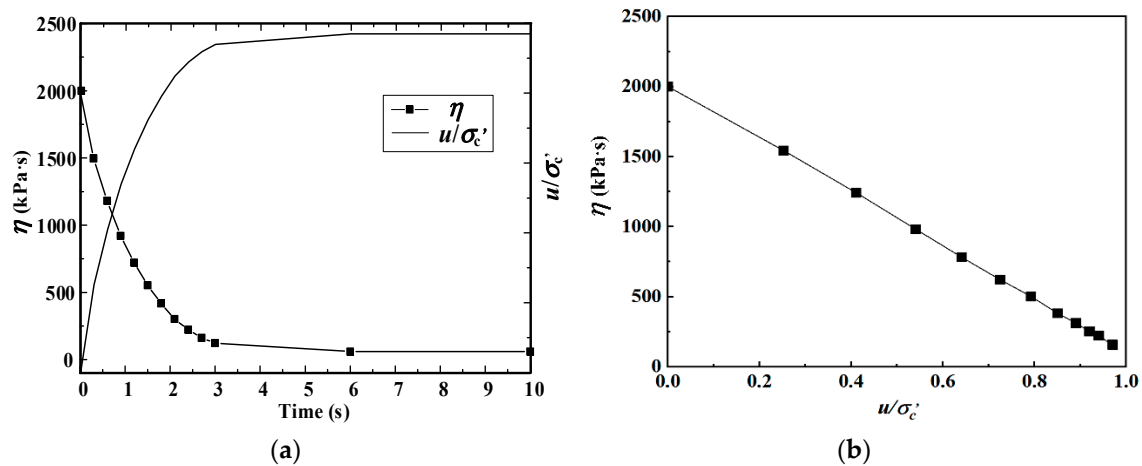


**Figure 5.** The excess pore pressure ratio and viscosity of soil. (a) Development of excess pore pressure ratio and viscosity coefficient. (b) Relationship between viscosity coefficient and excess pore pressure ratio.

### 3.3. Analysis Procedures

The computational analysis was separated into two stages: (1) Simulations were conducted to obtain the initial stress state of the soil by applying the gravity load to the convection–solid coupling model. The stress and strain of the model at this stage were used as the initial state applied at the dynamic analysis stage; (2) the dynamic analysis of the pile–soil interaction was conducted by applying a sine-wave load. In order to better obtain the dynamic interaction between the pile and soil during the accumulation of pore pressure, a sine-wave excitation with an acceleration amplitude of 0.2 g and a frequency of 2 Hz was used in this research. The flow field analysis used the improved Newton–Raphson arithmetic to deal with the system’s equation and the Newmark method for calculations. The time step was 0.01 s, with a total of 1000 steps.

### 3.4. Verification of the Method

The results of the pile’s dynamic displacement, the bending moment, and the soil’s accelerations from the numerical analysis were compared with that of the shake table test. The time history of displacement at the pile head is compared in Figure 6. The consequence indicates that the dynamic response of the proposed model generally agrees with that of the physical model. The displacement of the pile heads of the experiment and numerical simulation both increased at first and then decreased at the end of shaking. At about 2.8 s, the displacement of the pile head reached its maximum value, and the apparent viscosity of liquefiable soil was about 150 kPa·s. During the liquefaction process, there are three characteristics: (1) With continuous loading, the apparent viscosity of the fluid gradually decreases and finally tends to be stable. (2) The inclined surface slowly slows down during the shake progress and eventually tends to form a “horizontal surface”. (3) Along with the decrease in the inclination angle, the thrust of soil on the pile is weakened as a result of the decrease in the flow rate of the soil around the pile. Therefore, the displacement of the pile head gradually decreases after about 2.8 s under the combined influence of apparent viscosity and flow rate.

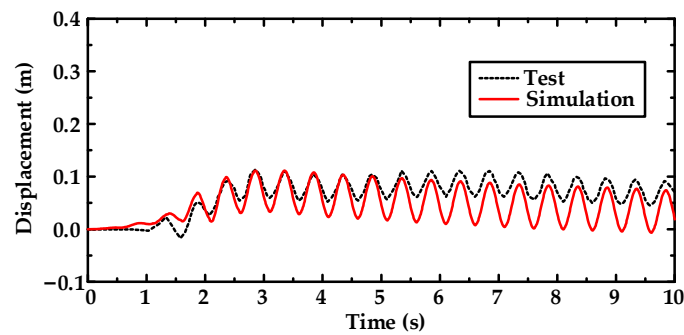


Figure 6. Time history of lateral displacement of rigid pile head.

The time history of bending moments of rigid piles measured at different depths is shown in Figure 7. The bending moments obtained by the numerical simulation were consistent with that of the experiment. The bending moment increased at the beginning of shaking and then gradually decreased after 4 s due to the reduction in apparent viscosity and flow rate of the liquefiable sand. Moreover, closer to the bottom of the model, a more pronounced increase in the bending moment of the pile was noted. The time at which the bending moment increased to its maximum value gradually decreased with the depth of the pile. There was a divergence between the tests and the experiments of the bending moment of the pile foundation of 6–10 s. The reason is that the constitutive model used in fluid mechanics ignores the spatial difference of apparent viscosity, which leads to the large apparent viscosity of the bottom after liquefaction and the relatively small apparent viscosity of the first liquefaction on the surface.

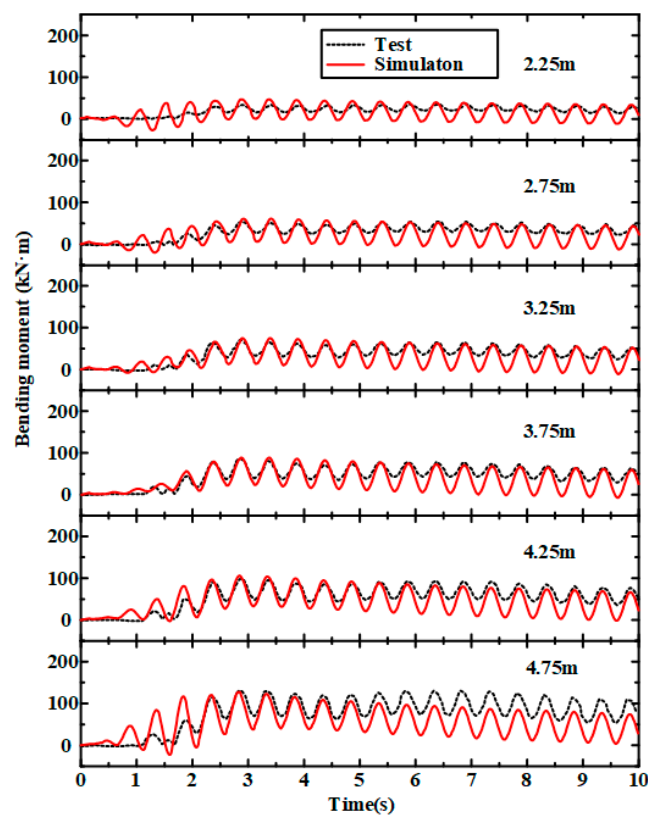
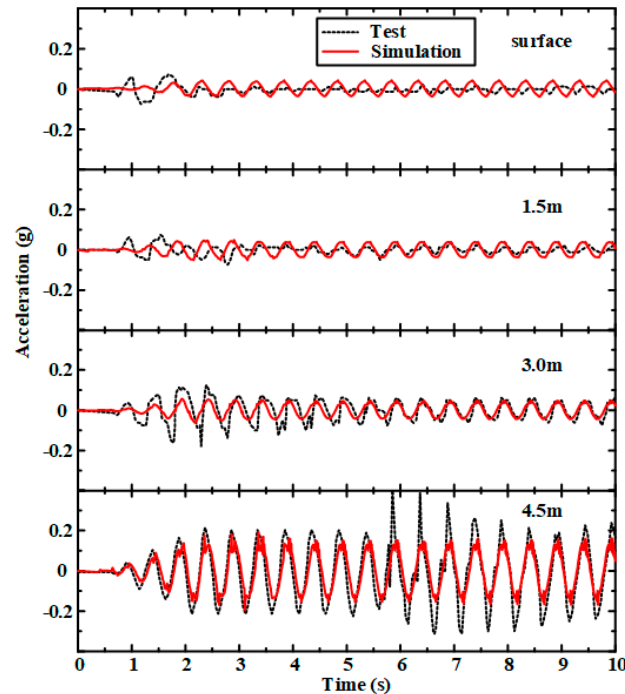


Figure 7. Bending moments time history curves of the rigid pile at different depths.

Figure 8 presents the time history of the acceleration of the soil at different depths. The accelerations of the soil exhibited a decreased amplitude near the surface, and the

acceleration amplitude in the loose sand after liquefaction was significantly reduced. This is due to the increase in the damping of liquefiable soil and the loss of stiffness and strength, which is related to the generation of excess pore water pressure.



**Figure 8.** Acceleration time history curves of soil at different depths.

For the results of the test, the soil surface is the first to be liquefied. The shake table test results show that the acceleration of the soil surface gradually decreases with the vibration time. Based on the numerical simulation of the fluid mechanics method, the attenuation phenomenon of soil surface acceleration is not obvious, which may be related to the apparent viscosity value when completely liquefied. On the other hand, the simulation results show that soil liquefaction has strong spatial nonlinearity. The apparent viscosity of the surface soil is very small during liquefaction, while the deep soil may not be liquefied. Similarly, if the soil layer is liquefied, the near-surface acceleration period increases slightly, and the natural frequency of the soil decreases.

#### 4. Parametric Analysis

Based on the fluid–solid coupling model of pile–soil interaction established between the two, the parameter influence analysis of pile–soil dynamic interactions in a liquefiable site was carried out, mainly considering the influence of elastic modulus and apparent viscosity and indirectly analyzing the influence of the site inclination angle on lateral flow and shear strain rate (expressed by loading frequency). The analysis parameters are shown in Table 2.

**Table 2.** Parametric analysis conditions.

Elastic Modulus	Apparent Viscosity	Site Inclination Angle	loading Frequency
$E$ (GPa)	$\eta$ (kPa·s)	$\alpha$ (°)	$f$ (Hz)
80	10	0	1.5
160	50	1	2
240	100	2	3
320	200	3	4

#### 4.1. Effect of Elastic Modulus of Pile

Four elastic moduli of 80 GPa, 160 GPa, 240 GPa, and 320 GPa were assigned to the pile to study its effect on pile–soil interactions in the liquefiable site. The distributions of the peak horizontal displacement and bending moments of the pile with depths for different elastic moduli are shown in Figure 9. The peak horizontal displacement of the pile foundation decreases with an increase in elastic modulus, and the distribution of bending moments along the depth was in contrast to the response of displacement.

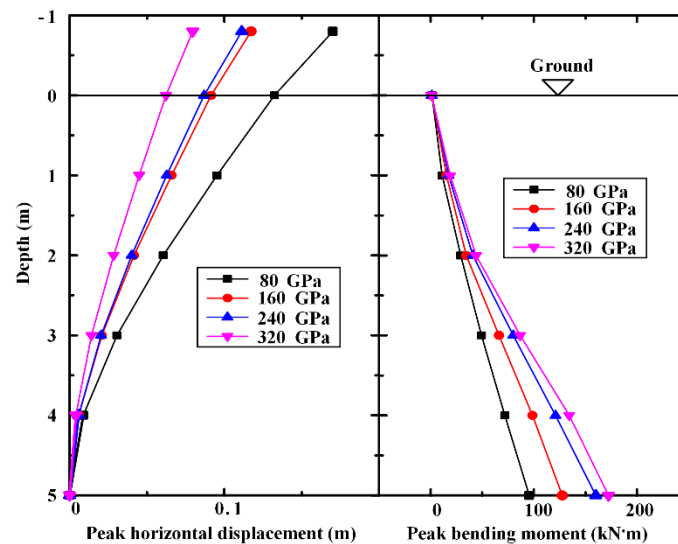


Figure 9. Effect of modulus of pile-on-pile responses.

#### 4.2. Effect of the Soil Apparent Viscosity

The apparent viscosity of liquefiable soil constantly decreases with the generation of excess pore pressure. To investigate the effect of apparent viscosity on the pile response, a horizontal site model without an inclination angle was established to eliminate the influence of the flow rate. Different apparent viscosities of the liquefied soil (10 kPa·s, 50 kPa·s, 100 kPa·s, and 200 kPa·s) were assigned in this study.

Figure 10 indicates the effect of apparent viscosity on the dynamic response of the pile. It can be seen that when the elastic modulus and loading frequency are constant, the peak bending moment and horizontal displacement of pile foundations increase with an increase in apparent viscosity. The greater the apparent viscosity, the closer the soil is to the solid state and the greater the dynamic soil thrust, resulting in an increase in the peak bending moment response. This is because the increase in dynamic earth pressure on the pile is related to the increase in soil modulus and strength.

During the liquefaction process, the shear deformation and acceleration of the soil change with the decrease in apparent viscosity. Figure 11 compares the acceleration of soil at different depths with different apparent viscosity. It could be observed that the amplitude of soil acceleration for the apparent viscosity of 200 kPa·s was larger than that for the apparent viscosity of 50 kPa·s. Moreover, the apparent viscosity also affects the phase difference of soil acceleration, and this phenomenon is more obvious near the surface of the model, which is essentially due to the fact that the ability of soil with different apparent viscosities to withstand shear deformation is different, which explains the filtering effect found in liquefied soils.

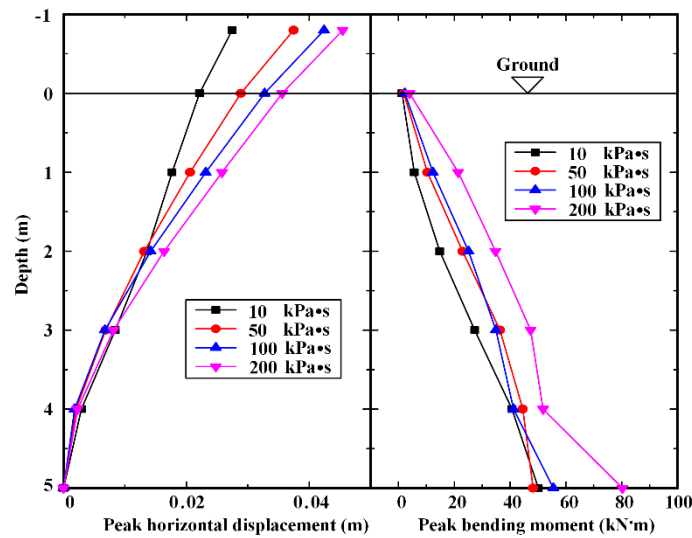


Figure 10. Influence of apparent viscosity on pile response.

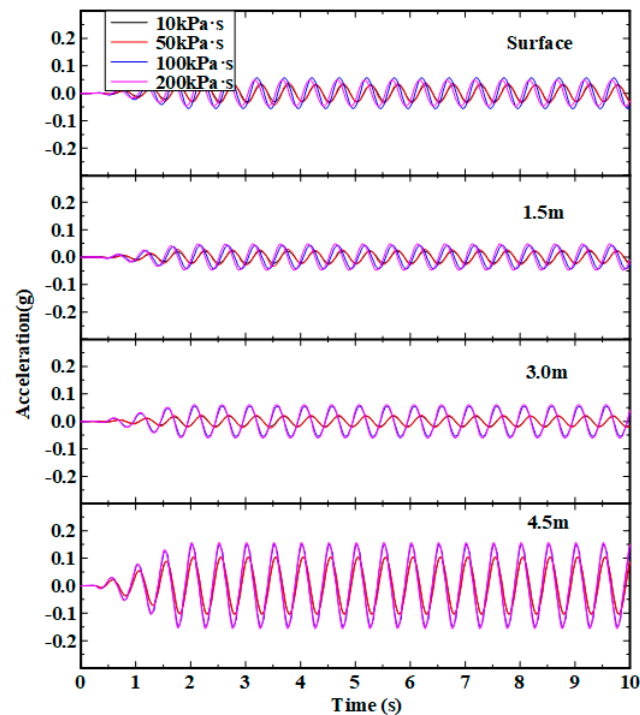


Figure 11. Influence of apparent viscosity on soil acceleration.

#### 4.3. Effect of the Site Inclination Angle

The inclination angle of the site will affect the shear strain rate of the liquefiable soil, thus affecting the pile–soil interaction. Similarly to the impact of water at different speeds on the pier, it will lead to differences in structural internal forces. In this study, four different inclination angles ( $0^\circ$ ,  $1^\circ$ ,  $2^\circ$ , and  $3^\circ$ ) were adopted to study the effect on dynamic responses of the pile foundation. The distribution of the peak horizontal displacement and bending moments along the depth for different inclination angles are presented in Figure 12. With the increase in inclination angle, the peak horizontal displacement response becomes larger, and the peak bending moment response of the pile foundation increases. The displacement and bending moment of the pile foundation are positively correlated with the lateral flow rate of soil around the pile, and the influence of the flow rate is more and more obvious.

The flow slip caused by soil liquefaction will cause additional load on the pile foundation, which will aggravate the dynamic response of the pile foundation.

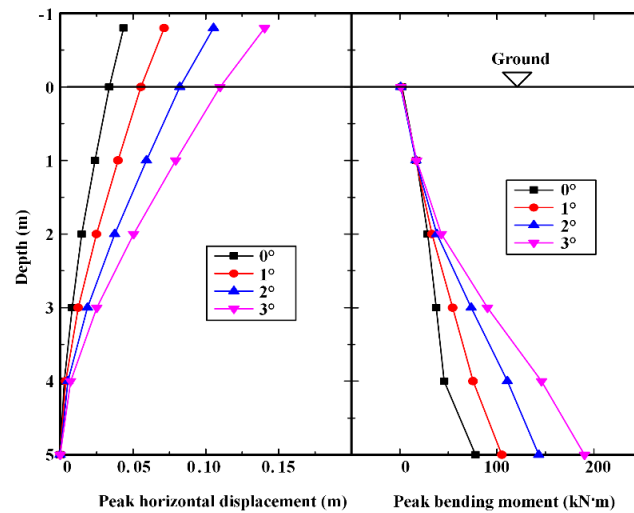


Figure 12. Effect of inclination angle on pile responses.

#### 4.4. Effect of Loading Frequency

Figure 13 shows the dynamic responses of the pile foundation under different loading frequencies. The peak horizontal displacement and bending moments of the pile foundation increase with a decrease in the loading frequency. The bending moment of the pile foundation reaches the maximum when the seismic frequency is 1.5 Hz. The reason for this phenomenon is that with the extension of continuous loading time, the apparent viscosity of the soil decreases gradually, the fluidity of the soil increases, and the shear strain rate increases. However, the soil also has a significant weakening effect on high-frequency ground motion, so the pile foundation response under high-frequency loads is small; that is, liquefied soil has the characteristics of amplifying low-frequency loads and filtering high-frequency loads.

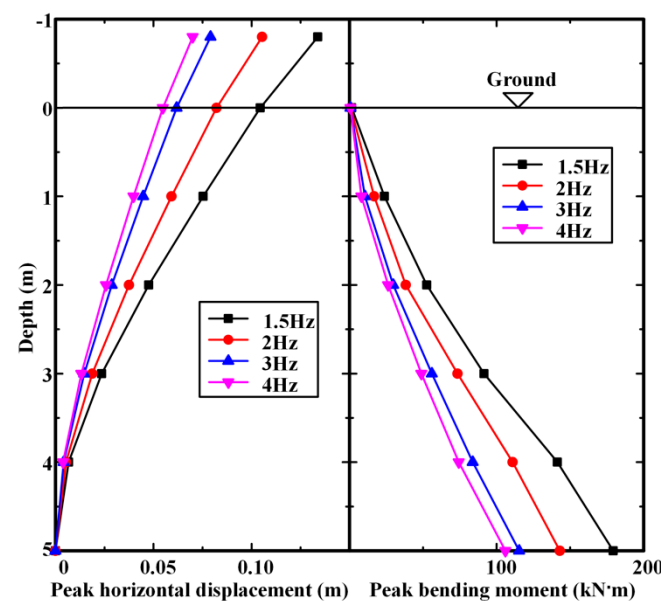


Figure 13. The responses of pile under different loading frequencies.

## 5. Conclusions

A pile–soil interaction analysis method that introduces the TEPP to represent the characteristics of liquefied soil is proposed. The proposed method was proven by comparing the calculated results with that of the shake table test. On this basis, the influencing factors including the elasticity coefficient of the pile, the apparent viscosity of the soil, the inclination angle of the site, and the loading frequency on the dynamic response of pile foundations were discussed. The main results are as follows.

- (1) The simulation results showed that the liquefaction characteristics of the soil were similar to that of thixotropic fluid as the pore pressure of the liquefaction can unify the periodic process. The experimental results showed that the pore pressure of liquefaction can simulate the soil after liquefaction, not only with respect to the flow characteristics but also the physical condition in advance of liquefaction.
- (2) The bending moments and lateral displacements of the pile, as well as the accelerations of the soil obtained by the numerical simulation, are consistent with that of the experiment. The peak horizontal displacement of pile foundations decreases with the elevation of the elastic modulus, and the distribution of bending moments along the depth was in contrast to the response of displacement.
- (3) The peak bending moment and horizontal displacement of pile foundations increase with the increase in apparent viscosity as a result of the increased dynamic earth pressure on the pile associated with the higher modulus and strength of the soil. With the increase in inclination angle, the peak horizontal displacement and bending moments of the pile foundation at all depths both increase due to the additional load on the pile foundation. The peak horizontal displacement and bending moments of the pile foundation increase with a decrease in the loading frequency as a result of the property of amplifying low-frequency loads and filtering high-frequency loads of liquefied soil.
- (4) The dynamic coupling interaction between liquefied soil and piles is closely related to the apparent viscosity of liquefied soil. The apparent viscosity could affect the amplitude of soil acceleration. Moreover, the apparent viscosity also affects the phase difference of soil acceleration, and this phenomenon is more obvious near the surface of the model due to the ability of soil with different apparent viscosities to withstand shear deformation being different, which explains the filtering effect found in liquefied soils.

**Author Contributions:** Conceptualization was done by X.Z. and Z.W.; methodology was performed by X.Z. and H.G.; software was provided by X.Z.; validation was performed by H.G. and Z.W.; formal analysis was performed by J.G.; investigation was performed by H.G. and J.G.; resources were provided by Z.W.; data curation was performed by Z.J.; original draft was written by X.Z. and Z.J.; reviewing and editing were done by Z.J.; visualization was performed by Z.J.; supervision was done by X.Z. All authors have read and agreed to the published version of the manuscript.

**Funding:** This study was supported by the National Natural Science Foundation of China (Grant No. 52178336 and 52108324). These financial supports are gratefully acknowledged. The contributions of anonymous reviewers and editors are also acknowledged.

**Institutional Review Board Statement:** Not applicable.

**Informed Consent Statement:** Not applicable.

**Data Availability Statement:** The data used to support the findings of this study are available from the corresponding author upon request.

**Conflicts of Interest:** No potential conflicts of interest were reported by the authors.

## References

1. Mallick, M.; Mandal, K.K.; Sahu, R.B. A Case Study of Liquefaction-Induced Damage to a Port Building Supported on Pile Foundation. In *Dynamics of Soil and Modelling of Geotechnical Problems*; Springer: Berlin/Heidelberg, Germany, 2022; pp. 319–330.
2. Tokimatsu, K.; Ishida, M.; Inoue, S. Challenge to Geotechnical Earthquake Engineering Frontier: Consideration of Buildings Overturned by the 2011 Tohoku Earthquake Tsunami. In *Proceedings of the 4th International Conference on Performance Based Design in Earthquake Geotechnical Engineering*, Beijing, China, 15–17 August 2022; pp. 580–596.
3. Yuan, J.; Wang, Y.; Zhan, B.; Yuan, X.; Wu, X.; Ma, J. Comprehensive investigation and analysis of liquefaction damage caused by the Ms7.4 Maduo earthquake in 2021 on the Tibetan Plateau, China. *Soil Dyn. Earthq. Eng.* **2022**, *155*, 107191. [[CrossRef](#)]
4. Rouholamin, M.; Lombardi, D.; Bhattacharya, S. Experimental investigation of transient bending moment of piles during seismic liquefaction. *Soil Dyn. Earthq. Eng.* **2022**, *157*, 107251. [[CrossRef](#)]
5. Liu, H. Seismic Damage of Tangshan Earthquake. *Seismol. Press* **1985**, *120*, 124–126. (In Chinese)
6. He, S.; Yan, S.; Deng, Y.; Liu, W. Impact protection of bridge piers against rockfall. *Bull. Eng. Geol. Environ.* **2019**, *78*, 2671–2680. [[CrossRef](#)]
7. Zhang, C.; Jiang, G.; Su, L.; Lei, D.; Liu, W.; Wang, Z. Large-scale shaking table model test on seismic performance of bridge-pile-foundation slope with anti-sliding piles: A case study. *Bull. Eng. Geol. Environ.* **2020**, *79*, 1429–1447. [[CrossRef](#)]
8. Zhang, C.; Jiang, G.; Lei, D.; Asghar, A.; Su, L.; Wang, Z. Large-scale shaking table test on seismic behaviour of anti-slide pile-reinforced bridge foundation and gravel landslide: A case study. *Bull. Eng. Geol. Environ.* **2021**, *80*, 1303–1316. [[CrossRef](#)]
9. Okamura, M.; Ono, K.; Arsyad, A.; Minaka, U.S.; Nurdin, S. Large-scale flow slide in Sibalaya caused by the 2018 Sulawesi earthquake. *Soils Found.* **2020**, *60*, 1050–1063. [[CrossRef](#)]
10. Chai, S.; Wang, L.; Wang, P.; Pu, X.; Xu, S.; Guo, H.; Wang, H. Failure Mechanism and Dynamic Response Characteristics of Loess Slopes Under the Effects of Earthquake and Groundwater. *Front. Multidiscip. Loess Geohazard Investig.* **2022**, *10*, 814740. [[CrossRef](#)]
11. Hussein, A.F.; El Naggar, M.H. Effect of model scale on helical piles response established from shake table tests. *Soil Dyn. Earthq. Eng.* **2022**, *152*, 107013. [[CrossRef](#)]
12. Zhang, D.; Wang, A.; Ding, X. Seismic response of pile groups improved with deep cement mixing columns in liquefiable sand: Shaking table tests. *Can. Geotech. J.* **2022**, *59*, 994–1006. [[CrossRef](#)]
13. Chen, Z.; Li, K.; Wang, C.; Ding, X.; Jiang, X.; Chen, Y. Shaking table tests on rigid-drainage pipe pile groups at liquefied laterally spreading site. *Eng. Mech.* **2022**, *39*, 141–152.
14. Kumar, R.; Sawaishi, M.; Horikoshi, K.; Takahashi, A. Centrifuge modeling of hybrid foundation to mitigate liquefaction-induced effects on shallow foundation resting on liquefiable ground. *Soils Found.* **2019**, *59*, 2083–2098. [[CrossRef](#)]
15. Ma, L.; Yang, K.; Yuan, W.; Li, L.; Wei, Y.; Ma, C.; Luo, F.; Zhang, G. Centrifuge modeling of the pile foundation reinforcement on slopes subjected to uneven settlement. *Bull. Eng. Geol. Environ.* **2020**, *79*, 2647–2658. [[CrossRef](#)]
16. Ashford, S.A.; Juirnarongrit, T.; Sugano, T.; Hamada, M. Soil–pile response to blast-induced lateral spreading. I: Field test. *J. Geotech. Geoenviron. Eng.* **2006**, *132*, 152–162. [[CrossRef](#)]
17. He, L.; Elgamal, A.; Abdoun, T.; Abe, A.; Dobry, R.; Hamada, M.; Menses, J.; Sato, M.; Shantz, T.; Tokimatsu, K. Liquefaction-induced lateral load on pile in a medium Dr Sand layer. *J. Earthq. Eng.* **2009**, *13*, 916–938. [[CrossRef](#)]
18. Zhuang, H.; Zhao, C.; Yu, X.; Chen, G. Earthquake responses of piles-soil dynamic interaction system for base-isolated structure system based on shaking table tests. *Chin. J. Geot. Eng.* **2022**, *44*, 979–987.
19. Broms, B.B. Lateral resistance of piles in cohesive soils. *J. Soil Mech. Found. Div.* **1964**, *90*, 27–63. [[CrossRef](#)]
20. Hamada, M.; Yasuda, S.; Isoyama, R.; Emoto, K. Observation of permanent ground displacements induced by soil liquefaction. *Doboku Gakkai Ronbunshu* **1986**, *1986*, 211–220. [[CrossRef](#)]
21. Wang, M.; Tobita, T.; Iai, S. Dynamic centrifuge tests of seismic responses of pile foundations in inclined liquefiable soils. *Chin. J. Rock Mech. Eng.* **2009**, *28*, 2012–2017.
22. Sun, J.; Li, X.; Gao, R.; Ren, Y.; Lu, T.; Pang, T. Numerical investigation of hydrolysis failure of aggregates in loess via CFD-DEM. *Environ. Geotech.* **2022**, *40*, 1–13. [[CrossRef](#)]
23. Wang, Z.; Ma, J.; Gao, H.; Stuedlein, A.W.; He, J.; Wang, B. Unified thixotropic fluid model for soil liquefaction. *Géotechnique* **2020**, *70*, 849–862. [[CrossRef](#)]
24. Hadush, S.; Yashima, A.; Uzuoka, R.; Moriguchi, S.; Sawada, K. Liquefaction induced lateral spread analysis using the CIP method. *Comput. Geotech.* **2001**, *28*, 549–574. [[CrossRef](#)]
25. He, L. *Liquefaction-Induced Lateral Spreading and Its Effects on Pile Foundations*; University of California: San Diego, CA, USA, 2005.
26. Kohno, H.; Bathe, K. A nine-node quadrilateral FCBI element for incompressible fluid flows. *Commun. Numer. Methods Eng.* **2006**, *22*, 917–931. [[CrossRef](#)]

**Disclaimer/Publisher’s Note:** The statements, opinions and data contained in all publications are solely those of the individual author(s) and contributor(s) and not of MDPI and/or the editor(s). MDPI and/or the editor(s) disclaim responsibility for any injury to people or property resulting from any ideas, methods, instructions or products referred to in the content.